Phase behavior of lipid mixtures based on human ceramides: coexistence of crystalline and liquid phases

J. A. Bouwstra,[1],* G. S. Gooris,* F. E. R. Dubbelaar,* and M. Ponec[†]

Leiden/Amsterdam Center for Drug Research,* Gorlaeus Laboratories, Leiden University, P.O. Box 9502, 2300 RA Leiden, The Netherlands; and Department of Dermatology,[†] Leiden University Medical Center, Leiden, The Netherlands

Abstract The lipid regions in the outermost layer of the skin (stratum corneum) form the main barrier for diffusion of substances through the skin. In this layer the main lipid classes are ceramides, cholesterol (CHOL), and FFA. Previous studies revealed a coexistence of two crystalline lamellar phases with periodicities of approximately 13 nm (referred to as long periodicity phase) and 6 nm (short periodicity phase). Additional studies showed that lipid mixtures prepared with isolated pig ceramides (pigCER) mimic lipid phase behavior in stratum corneum closely. Because the molecular structure of pigCER differs in some important aspects from that of human ceramides (HCER), in the present study the phase behavior of mixtures prepared with HCER has been examined. Phase behavior studies of mixtures based on HCER revealed that in CHOL:HCER mixtures the long periodicity phase dominates. In the absence of HCER1 the short periodicity phase is dominant. Addition of FFA promotes the formation of the short periodicity phase and induces a transition from a hexagonal sublattice to an orthorhombic sublattice. Furthermore, the presence of FFA promotes the formation of a liquid phase. Finally, cholesterol sulfate, a minor but important lipid in the stratum corneum, reduces the amount of cholesterol that phase separates in crystalline domains. From these observations it can be concluded that the phase behavior of mixtures prepared from HCER differs in some important aspects from that prepared from pigCER. The most prevalent differences are the following: i) the addition of FFA promotes the formation of the short periodicity phase; and ii) liquid lateral packing is obviously present in CHOL:HCER:FFA mixtures. These changes in phase behavior might be due to a larger amount of linoleic acid moiety in HCER mixtures compared with that in pigCER mixtures.—Bouwstra, J. A., G. S. Gooris, F. E. R. Dubbelaar, and M. Ponec. **Phase behavior of lipid mixtures based on human ceramides: coexistence of crystalline and liquid phases.** *J. Lipid Res.* 2001. **42: 1759–1770.**

Supplementary key words skin • X-ray diffraction • lipid organization

The most important natural function of the mammalian epidermis is to act as a barrier against unwanted influences from the environment. It has been known for many years that the outermost layer of the skin [the densely packed stratum corneum (SC)] acts as the main barrier between the interior milieu and the external environment. The SC consists of keratin-filled cells, referred to as corneocytes, which are embedded in a crystalline lipid lamellar matrix. The lipid regions in the SC form the only continuous domain. Because the cornified envelope of the corneocytes is almost impermeable to diffusing substances, the main penetration pathway of substances through the SC is located in the intercellular lipid matrix. For this reason the physical properties of the SC lipids are considered to be important for proper skin barrier function. The lipid composition differs markedly from that of typical biological membranes. The predominant lipid classes are ceramides (CER), cholesterol (CHOL), and FFA.

X-ray diffraction studies revealed that in pig and human SC two crystalline lipid lamellar phases with periodicities of approximately 6 nm [referred to as the short periodicity phase (SPP)] and 13 nm [referred to as the long periodicity phase (LPP)], respectively (1–4), coexist. In mouse and human SC the lipids are predominantly organized in an orthorhombic lateral sublattice (1, 3, 5, 6), whereas in pig SC the lipids form a hexagonal sublattice (4). Because only the liquid phase is common in biological membranes and the 13 nm periodicity is not observed in phospholipid systems, the lipid organization in SC is unusual. Because the 13 nm lamellar phase is present in all examined species and is of an unusual lipid arrangement (7), this phase has been considered to be important for the permeability barrier of the skin.

To obtain detailed insight concerning the role the various lipid classes play in the barrier function of the skin, various studies with lipid mixtures have been performed. It appeared that lipid mixtures based on brain CER, CHOL,

---

and palmitic acid formed mainly crystalline phases (8, 9) with a small fraction of lipids forming more mobile phases. However, in lipid mixtures containing CHOL, palmitic acid and brain CER only the SPP has been formed (10). Additional studies by Moore, Rerek, and Mendelsohn (11, 12) confirmed the presence of crystalline phases in CHOL, palmitic acid, and either bovine brain CER mixtures or mixtures prepared from synthetic CER 2 or 5. Several X-ray diffraction studies have been carried out with mixtures containing CER isolated from pig SC (pigCER). These studies showed that mixtures prepared from isolated pigCER and CHOL form two lamellar phases with periodicities of 12.2 and 5.2 nm, mimicking the lamellar phases in intact porcine SC.

The CHOL:pigCER mixtures form a hexagonal lateral sublattice (13), which is present in pig SC, but not in human SC. Addition of long chain FFA increased the periodicities of the lamellar phases slightly and induced a phase transition from a hexagonal sublattice to an orthorhombic sublattice (14). From these studies it was concluded that the presence of CER and CHOL is important for the formation of the lamellar phases, whereas long chain FFA increase the density of the hydrocarbon chain packing. In studies using Fourier-transformed infrared (FTIR) spectroscopy (15) it has been suggested that in intact human and pig SC a subpopulation of lipids forms a liquid phase. The finding that no liquid phase has been observed in CHOL:pigCER:FFA mixtures with the X-ray diffraction technique is seemingly in contrast with the FTIR results (15).

In native SC, next to the major SC lipids the presence of minor lipids, such as cholesterol sulfate, and the existence of a pH and calcium gradient may affect the final organization of SC lipids. It has been observed that addition of cholesterol sulfate to CHOL:pigCER:FFA mixtures induced the formation of liquid lateral packing and increased the solubility of CHOL in the lamellar phases. Furthermore, cholesterol sulfate promoted the formation of the 13 nm lamellar phase (14, 16). The presence of calcium counteracted the effect of cholesterol sulfate. Several studies report the existence of a pH gradient in SC. The pH is approximately 5–6 at the skin surface and 7.4 at the SG-stratum granulosum interface (17–19). In mixtures containing pigCER an increase in pH promoted the presence of the 13 nm phase, as observed after the addition of cholesterol sulfate.

Until now most of the studies have been performed with brain or pigCER. Because the molecular structures of pigCER and human CER (HCER) differ (**Fig. 1**) it is of great importance to gain information about the phase behavior of mixtures based on HCER. This will help us understand the changes in barrier function and lipid organization in diseased and dry skin. In human SC at least eight subclasses of CER are present (20, 21). These HCER, often
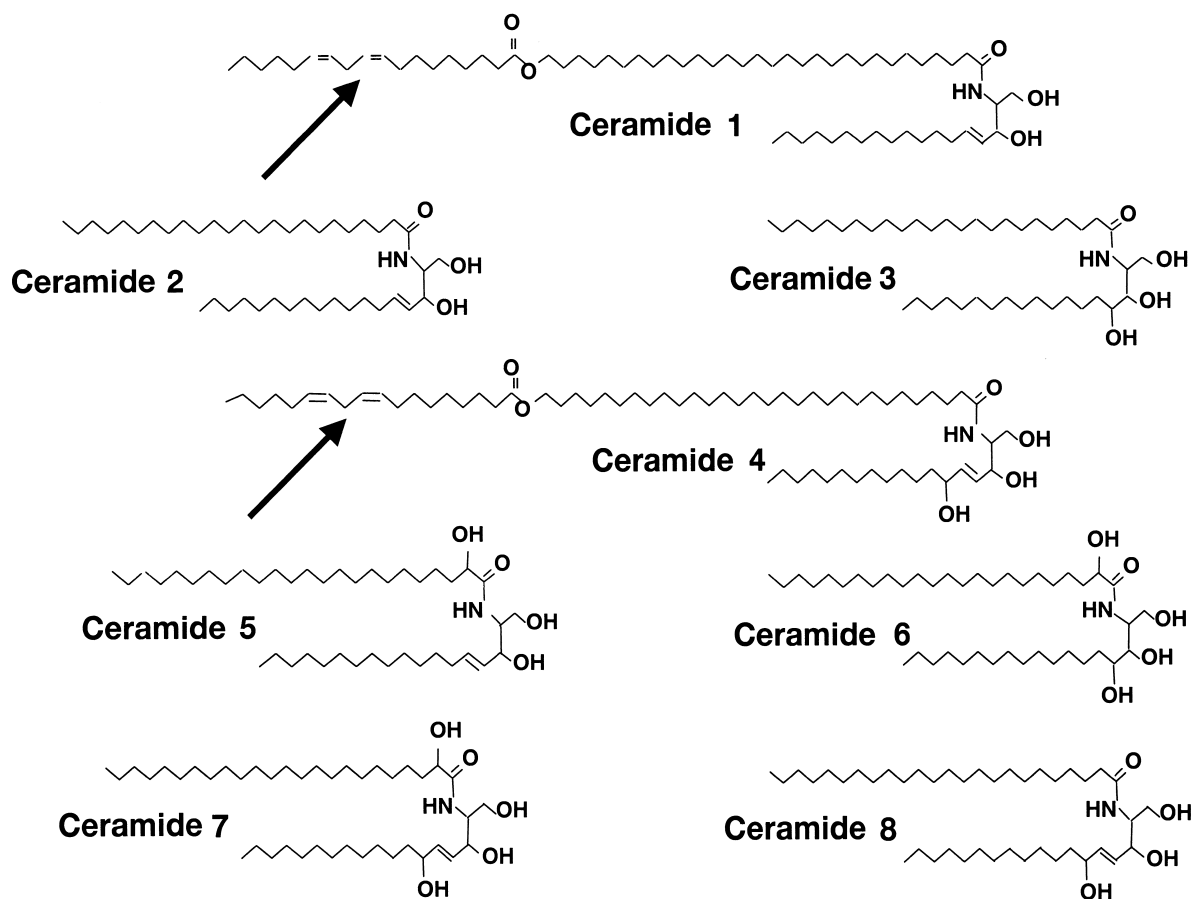

Fig. 1. The molecular structure of human CER. Arrows: linoleate of HCER1 and of HCER4.

referred to as HCER1 to HCER8, differ from each other in head group architecture and hydrocarbon chain length. HCER1 and HCER4 both possess an exceptional molecular structure: a linoleic acid is linked to a ω-hydroxy fatty acid with a chain length of approximately 30–34 carbon atoms. In this respect the HCER are different from pigCER, of which only pigCER1 has this exceptional molecular structure (22).

The aim of the present study was to investigate the lipid phase behavior of mixtures prepared with HCER and to focus on the role of HCER, CHOL, FFA, and cholesterol sulfate. Because in pigCER mixtures the role of cholesterol sulfate was counteracted by calcium, the effect of calcium in cholesterol sulfate-containing mixtures was studied as well. In addition, we have varied the pH (pH 5 vs. 7.4) to examine whether a pH gradient in SC plays a role in lipid phase behavior. Because in pigCER mixtures HCER1 was found to play a crucial role in the formation of the LPP, the phase behavior was also studied with HCER mixtures lacking HCER1.

MATERIALS AND METHODS

Extraction, separation, and identification of lipids from SC

Human abdomen or mammary skin was obtained after cosmetic surgery and processed the same day. The subcutaneous fat was removed and the skin was dermatomed to a thickness of approximately 250–300 μm (Padgett Dermatome, Kansas City, MO). To obtain SC dermatomed skin was incubated with its dermal side on Whatman (Clifton, NJ) paper soaked in a solution of 0.1% (w/v) trypsin (Sigma, Zwijndrecht, Netherlands) in 0.15 M PBS (NaCl, 8 g/l; KCl, 0.19 g/l; KH_2PO_4, 0.2 g/l; Na_2HPO_4, 1 g/l) overnight at 4°C and for 1 h at 37°C. After this the SC was peeled away from the epidermis and dermis. Epidermal lipids were extracted according to the method of Bligh and Dyer (23). The extracted lipids were applied on a silicagel 60 (Merck, Darmstadt, Germany) column with a diameter of 2 cm and a length of 33 cm. The various lipid classes were eluted sequentially, using various solvent mixtures as published previously (13). The lipid composition of collected fractions was established by one-dimensional high performance thin-layer chromatography, as described earlier (24). For quantification, authentic standards (Sigma) were run in parallel. The quantification was performed after charring, using a photodensitometer with peak integration (GS 710; Bio-Rad, Hercules, CA). Isolated HCER fractions have been mixed to achieve a composition similar to that of human SC.

Preparation of lipid mixtures

Various classes of lipids were mixed in various molar ratios, using a mean HCER molar weight of 700. Mixtures were prepared from either *i*) CHOL and HCER, *ii*) CHOL, HCER, and FFA, *iii*) CHOL, HCER, FFA, and cholesterol sulfate, *iv*) CHOL, HCER, FFA, cholesterol sulfate, and $CaCl_2$, or *v*) CHOL and HCER in the absence of HCER1 [referred to as HCER(2–8)].

For the FFA we chose a mixture of long chain FFA with a composition similar to that present in SC (25). The fatty acid composition was $C_{16:0}$, $C_{18:0}$, $C_{22:0}$, $C_{24:0}$, and $C_{26:0}$ in the molar ratio 1:3:42:37:7. The mixtures were prepared at either pH 5, which is the approximate pH at the skin surface, or at pH 7.4, the pH at the SC-stratum granulosum interface (17, 18). To achieve a pH of 5 an acetate buffer was used; to prepare mixtures at a pH of

7.4 a HEPES buffer was used. A detailed description of the lipid mixture preparation is given elsewhere (13). Briefly, approximately 2 mg of lipids was dissolved in chloroform–methanol 2:1 (v/v) at the desired composition and applied to mica. The organic solvent was evaporated under a steam of nitrogen, after which the sample was heated to 60°C. After equilibration for 10 min, the lipid mixtures were covered with 1–2 ml of buffer at pH 5.0 and cooled. Subsequently at least 10 freeze-thawing cycles were carried out.

Diffraction methods

Small-angle X-ray diffraction. All measurements were carried out at the synchrotron radiation source at Daresbury Laboratory (Daresbury, Warrington, Cheshire, UK), using station 8.2. The samples were placed in a specially designed sample holder with two mica windows. A detailed description of the equipment has been given elsewhere (2). The experimental conditions were similar to those described previously (13). The scattered intensities were measured as a function of θ, the scattering angle. Calibration of the detector was carried out with rat tail and CHOL. From the scattering angle the scattering vector (Q) was calculated as $Q = 4\pi(\sin \theta)/\lambda$, in which λ is the wavelength, being 0.154 nm at the sample position.

A lamellar phase is characterized by a series of peaks at equidistant positions in the diffraction curve. The positions of the diffraction peaks are directly related to the periodicity d, namely $d = 2n\pi/Q_n$, in which n is the order of the diffraction peak. Each peak is referred to by its spacing, which is equal to $2\pi/Q_n$. The intensities of the various diffraction curves of the samples were scaled by using the tail of the diffraction curve.

For some samples the diffraction curves were measured as a function of temperature. The temperature was gradually increased with a heating rate of 2°C/min. Data collection was carried out continuously. Each minute a new diffraction curve was collected. In this way each successive set of diffraction data reflects the mean lipid organization over a temperature rise of 2°C.

Wide-angle X-ray diffraction. The diffraction patterns were obtained at room temperature with a fiber diffraction camera at station 7.2 of the synchrotron radiation source in Daresbury. A more detailed description of the equipment is given elsewhere (6). The X-ray path length through the sample was approximately 1 mm. The sample-to-film distance was set to 0.11 m. The wavelength of the X-rays was 0.1488 nm. To obtain a high resolution in the wide-angle X-ray diffraction (WAXD) pattern a cross-section of the primary beam was adjusted to 300 μm². The X-rays were collected over 2–4 min by an image plate (two-dimensional detection). To obtain an improved signal-to-noise ratio, the detected X-rays were integrated over an angle of 360°. The temperature-induced phase transitions of HCER:CHOL:FFA and pigCER:CHOL:FFA mixtures have been compared. To do so the diffraction patterns were measured statically at selected temperatures.

RESULTS

Lipid composition

The CER composition as determined by high performance thin-layer chromatography was 9.4% (HCER1), 31.7% (HCER2), 21.6% (HCER3), 8.4% (HCER4), 13.4% (HCER5+HCER6+HCER8), 15.3% (HCER7).

Lateral packing

Explanation of reflections. Liquid packing is characterized by a broad reflection at approximately 0.46 nm. In gen-

eral, the strongest reflection in the pattern of the hexagonal lateral packing is located at approximately 0.41 nm. The diffraction pattern of the orthorhombic lateral packing is characterized by two strong reflections at an approximate spacing of 0.41 and 0.37 nm.

CHOL:HCER mixtures. In **Fig. 2A** the diffraction pattern of an equimolar CHOL:HCER mixture is depicted. The pattern is characterized by a large number of strong and weak peaks. A strong peak at a spacing of 0.407 nm indicates the presence of a hexagonal sublattice. In addition, a series of sharp peaks ranging mainly between 0.6 and 0.41 nm can be attributed to crystalline CHOL. Whether a liquid phase is present cannot be deduced from this pattern. This is due to the high number of CHOL reflections that obscure the broad reflection at 0.46 nm of the liquid phase. Therefore, it was decided to scan the entire sample to select a region at which the crystalline CHOL reflections were not dominating. The WAXD pattern (not shown) obtained from a region that contained less crystalline CHOL revealed that a subpopulation of lipids forms a liquid phase. Furthermore, the sixth order of the 12.8 nm lamellar phase and the fourth order and/or ninth order of the 5.4 and 12.8 nm phases, respectively, are present. These reflections are at approximately the same position and therefore cannot be distinguished.

A reduction of the CHOL:HCER ratio from 1:1 to 0.2:1 does not affect the position of the 0.406 nm peak, indicating that the hexagonal lateral packing is not sensitive to the changes in CHOL:HCER molar ratio. As expected, a decrease in the CHOL:HCER molar ratio to 0.6 and 0.2 reduces the intensity of the peaks attributed to crystalline CHOL. At a CHOL:HCER molar ratio of 0.6 a broad shoulder is present at approximately 0.46 nm (Fig. 2B). This indicates the presence of a liquid phase, also at lower CHOL contents.

CHOL:HCER(2–8) mixtures. The diffraction pattern of the CHOL:HCER(2–8) mixtures indicates the formation of hexagonal lateral packing next to the appearance of the crystalline CHOL; see Fig. 2C. Higher order reflections of the two lamellar phases are indicated in Fig. 2C.
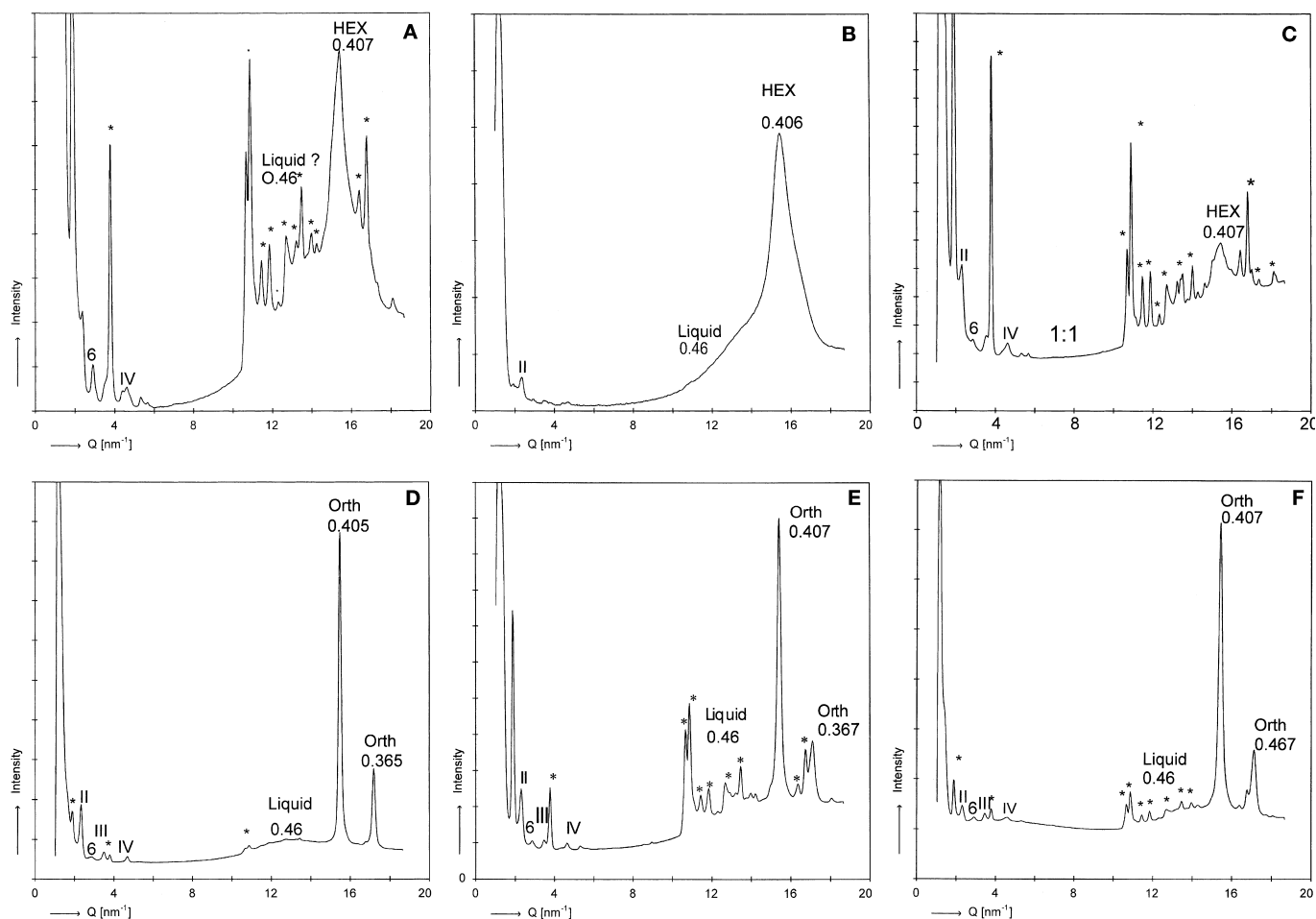

Fig. 2. The lateral packing of CHOL:HCER and CHOL:HCER:FFA mixtures. HEX, Orth, and Liquid denote reflections attributed to hexagonal, orthorhombic, and liquid lateral packing, respectively. An asterisk indicates a reflection attributed to crystalline CHOL. The Arabic numbers indicate the diffraction orders of the long periodicity. The Roman numbers indicate the diffraction orders of the SPP. A: CHOL:HCER, 1:1. B: CHOL:HCER, 0.6:1. C: CHOL:HCER(2–8), 1:1. D: CHOL:HCER:FFA, 1:1:1. E: CHOL:HCER:FFA, 1:1:0.4. F: CHOL:HCER:FFA, 1:1:1. In this mixture 50% long chain FFA has been replaced by palmitic acid.

CHOL:HCER:FFA mixtures. In the diffraction pattern of the equimolar CHOL:HCER:FFA mixture (Fig. 2D) the intensity of the peaks attributed to CHOL is strongly reduced compared with the mixtures that do not contain FFA. Furthermore, the presence of two peaks at 0.405 and 0.365 nm indicates the formation of an orthorhombic phase. Remarkable is the presence of a broad peak at approximately 0.46 nm, indicating the presence of a liquid phase. Addition of cholesterol sulfate or cholesterol sulfate plus calcium does not affect the lateral packing strongly (not shown). Finally, higher order reflections of the 12.8 and 5.4 nm lamellar phases can clearly be detected.

A reduction in FFA content in the CHOL:HCER:FFA mixtures to 1:1:0.8 does not affect the lateral packing. However, the intensities of the peaks attributed to CHOL slightly increase, indicating a decreased CHOL solubility in these lattices. The orthorhombic lateral packing persists even after a reduction in FFA content to form a 1:1:0.4 CHOL:HCER:FFA ratio (Fig. 2E).

We also examined whether the fatty acid chain length affects the formation of the lateral sublattice by substitution of about 50% of the long chain FFA by palmitic acid. This replacement did not affect the lateral packing. The presence of a peak at 0.46 nm indicates that a liquid phase coexists with orthorhombic lateral packing (Fig. 2F).

Finally, the lipid phase behavior of equimolar CHOL:HCER:FFA mixtures has been studied not only at pH 5, but also at pH 7.4. An increase in pH did not affect the lateral packing; again, a liquid lattice and an orthorhombic lattice coexisted (not shown).

CHOL:HCER:FFA mixtures at elevated temperature. The X-ray dif-

fraction of the equimolar CHOL:HCER:FFA mixture has been measured statically at 32°C, 37°C, 42°C, 60°C, and 72°C. At 32°C the lateral packing (see **Fig. 3**) is already different from that observed at room temperature. Two peaks are observed at 0.409 and 0.376 nm. These peaks cannot be attributed to either an orthorhombic phase (spacings at 0.406 and 0.365 nm) or a hexagonal phase (one spacing at 0.409 nm). A further increase in temperature to 37°C revealed the presence of hexagonal lateral packing (not shown). Possibly between room temperature and 37°C a change from orthorhombic packing to a hexagonal phase occurs with a pseudo-hexagonal phase as intermediate phase, as observed in aliphatic hydrocarbons (26). This phase is indeed characterized by two spacings, of which the shortest spacing is located in between the two spacings characteristic of the orthorhombic phase. A gradual change in peak position from 0.365 to 0.406 nm has also been observed in intact human SC (27) and in isolated pigCER mixtures (J. A. Bouwstra, G. S. Gooris, F. E. R. Dubbelaar, and M. Ponec, unpublished results). A further increase in temperature to 42°C reduces the spacing of the hexagonal packing slightly to 0.403 nm, after which the spacing increases to 0.406 nm at 60°C and to 0.41 nm at 72°C. At this temperature the intensity of the 0.41 nm peak is strongly reduced. Simultaneously, the intensity of the broad reflection at 0.46 nm increases strongly, indicating a transition from a hexagonal to a liquid phase.

Lamellar phases

CHOL:HCER mixtures. The diffraction curves of the CHOL:HCER mixtures are given in **Fig. 4A**. In the diffraction curve of the equimolar CHOL:HCER mixture the peaks located at a spacing of 13, 6.2, 4.5, 2.2, and 1.89 nm are attributed to a long periodicity lamellar phase (first, second, third, sixth, and seventh order) with a repeat distance of 12.8 nm. Whether an SPP is also present in the mixture is not obvious from the diffraction pattern, because the 5.4 nm peak, which is the first order reflection of the 5.4 nm phase clearly detected in diffraction patterns of CHOL:pigCER mixtures (13), is not present. However, some indications of the presence of the SPP can be deduced from the pattern, namely *i)* the spacing of the 2.7 nm peak is slightly too long for being a fifth order reflection of the 12.8 nm lamellar phase. Possibly the 2.7 nm peak is the second order reflection of the 5.4 nm phase; and *ii)* the 4.5 nm peak is slightly asymmetric, indicating that it might obscure the presence of a weak 5.4 nm peak. In addition, peaks at a spacing of 3.33 and 1.69 nm are attributed to crystalline CHOL present in separate domains. A reduction in CHOL level to a 0.6 and 0.2 molar ratio reduces the intensities of the 3.33 and 1.69 nm peaks, but does not markedly change the positions of the peaks attributed to the lamellar phases.

CHOL:HCER(2–8) mixture. The diffraction curve of the equimolar CHOL:HCER(2–8) mixture reveals a strong 5.3 nm peak and two weaker peaks at 6.4 and 4.4 nm and a weak reflection at 2.65 nm. This indicates that the lipids form mainly a 5.3 nm phase and that only a small fraction of lipids forms a lamellar phase with a periodicity of ap-
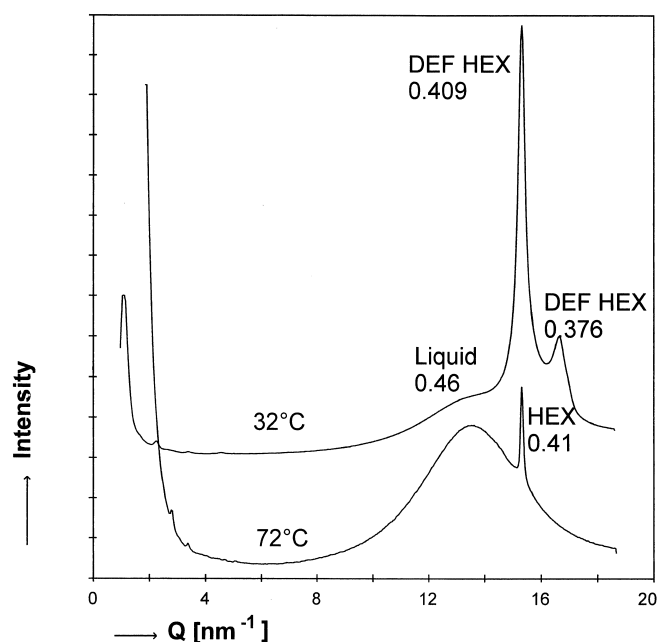

Fig. 3. The wide-angle diffraction curves of an equimolar CHOL:HCER:FFA mixture monitored at 32°C and 72°C. At 32°C two peaks are observed at 0.409 and 0.376 nm, indicating that a pseudo-hexagonal phase (DEF HEX) coexists with a liquid phase. At 72°C the hexagonal lateral packing almost disappears at the expense of the liquid phase.
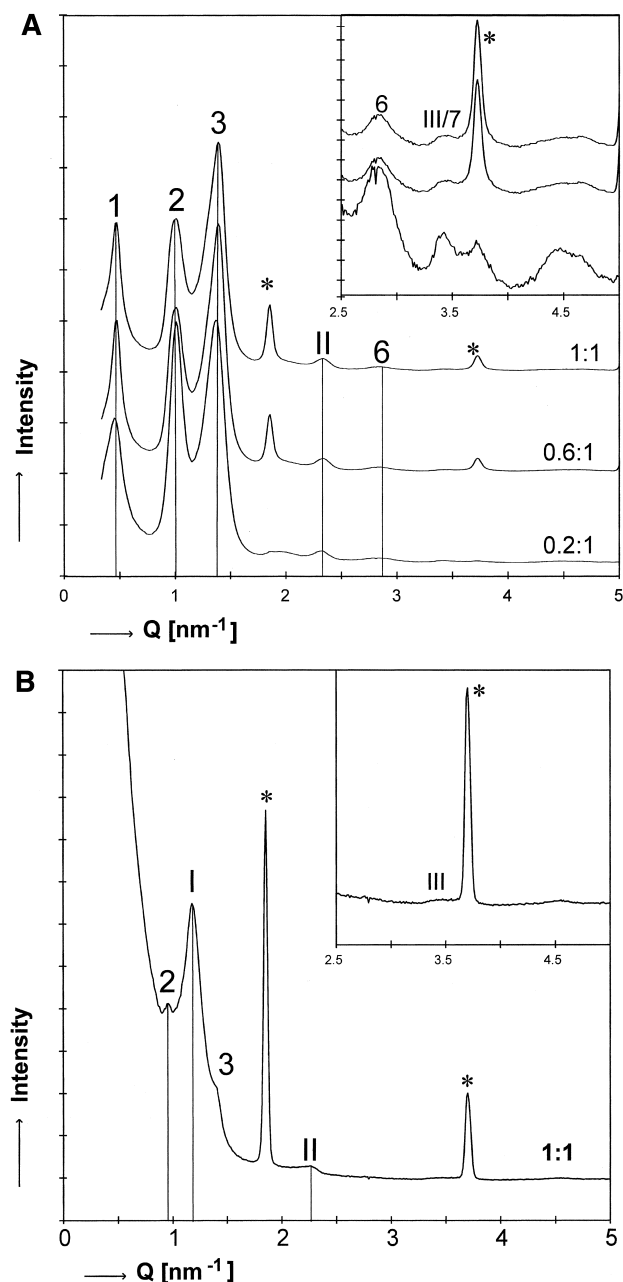
Fig. 4. The phase behavior of CHOL:HCER and CHOL:HCER (2–8) mixtures. The Arabic numbers indicate the diffraction orders of the LPP (repeat distance, 12.8 nm). The Roman numbers indicate the diffraction orders of the SPP (repeat distance, 5.4 nm). * Peaks located at spacings of 3.33 nm ($Q = 1.86$ nm^{-1}) and 1.69 nm ($Q = 3.74$ nm^{-1}) are attributed to crystalline CHOL present in separate domains. A: The effect of CHOL:HCER molar ratio on the phase behavior at pH 5. In the diffraction curve the peaks located at a spacing of 13 nm ($Q = 0.48$ nm^{-1}), 6.2 nm ($Q = 1.01$ nm^{-1}), 4.5 nm ($Q = 1.39$ nm^{-1}), 2.2 nm ($Q = 2.85$ nm^{-1}), and 1.89 nm ($Q = 3.32$ nm^{-1}) are attributed to a long periodicity lamellar phase (first, second, third, sixth, and seventh order) with a repeat distance of 12.8 nm. The presence of the SPP can be deduced from the spacing at the 2.7 nm peak ($Q = 2.32$ nm^{-1}, second order) and the asymmetry of the 4.5 nm peak. B: The diffraction profile of the equimolar CHOL:HCER(2–8) mixture at pH 5. The diffraction curve of the equimolar CHOL:HCER(2–8) mixture reveals a strong 5.3 nm peak ($Q = 1.19$ nm^{-1}, first order) and a weak peak at 2.65 nm ($Q = 2.37$ nm^{-1}, second order) of the 5.4 nm phase. Two weak peaks at 6.4 nm ($Q = 0.98$ nm^{-1}, second order) and 4.4 nm ($Q = 1.43$ nm^{-1}, third order) are attributed to the 12.8 nm lamellar phase.

proximately 13 nm (Fig. 4B). The strong peaks at 3.37 and 1.69 nm reveal that a substantial fraction of the CHOL phase separates in crystalline domains.

CHOL:HCER:FFA mixtures. The phase behavior of the equimolar CHOL:HCER:FFA mixture at pH 5 is shown in **Fig. 5**. A short 5.5 nm lamellar phase is present in the mixture. This can be deduced from the presence of the peaks at spacings of 5.5 nm (first order), 2.77 nm (second order), 1.85 nm (third order), and 1.35 nm (fourth order). The 13 nm lamellar phase is also present in the mixture. Namely, at both sides of the 5.5 nm peak a shoulder is present with spacings of 6.2 nm (second order) and 4.5 nm (third order). In addition, the 2.23 nm peak is a sixth order reflection of the 13 nm phase. Furthermore, the peaks at 1.85 and 1.38 nm attributed to the 5.5 nm phase might also be attributed to the 13 nm lamellar phase (seventh and ninth order). Two peaks at 3.39 and 1.69 nm spacings are due to crystalline CHOL. Reduction in the FFA content does not change the phase behavior significantly (not shown), except that the shoulders on the strong 5.5 nm peak ($Q = 1.14$ nm^{-1}) are less prominent as compared with those seen in the equimolar CHOL:HCER:FFA mixture. After addition of cholesterol sulfate the CHOL reflections disappear, indicating that cholesterol sulfate facilitates the intercalation of CHOL in the lamellar phases (Fig. 5). Furthermore, addition of cholesterol sulfate makes the detection of the peaks attributed to the LPP more difficult. On the basis of the broad 3.4 nm (fourth order), 2.31 nm (sixth order), and 1.85 nm (seventh order) reflections, it is likely that a small fraction of lipids forms the 13 nm lamellar phase. Most probably the 4.3 and 6.2 nm shoulders, clearly present in the pattern of the equimolar CHOL:CER:FFA mixture, cannot be detected after addition of cholesterol sulfate because of an increase in width of the peaks. The presence of a broad strong peak at 5.6 nm spacing clearly shows that a large fraction of lipids forms the SPP. However, the LPP is still present as indicated by the broad peaks at 3.3 and 2.2 nm (fourth and sixth order of this phase). Most probably the second and third order peaks of the LPP are weak and broad and can therefore not be distinguished from the broad 5.6 nm peak.

Preparation of the lipid mixtures in the presence of calcium does not change the lipid phase behavior. The diffraction peak at spacings of 5.6 nm (first order), 1.85 nm (third order) and 1.37 nm (fourth order) are attributed to a phase with a periodicity of 5.6 nm. Broad peaks at 3.3 (fourth order) nm and 2.2 (sixth order) nm indicate again the presence of the 13 nm phase. Furthermore, the seventh order peak of the LPP and the fourth order peak of the SPP are separated because of a sharpening of the peaks attributed to the 13 nm phase. Possibly the 1.37 nm reflections can also be attributed to the 13 nm phase.

The phase behavior of the equimolar lipid mixtures at pH 7.4 has also been measured in the presence and absence of cholesterol sulfate. The inspection of the diffraction patterns revealed that the lipid organization at pH 7.4 is similar to that at pH 5 (not shown).

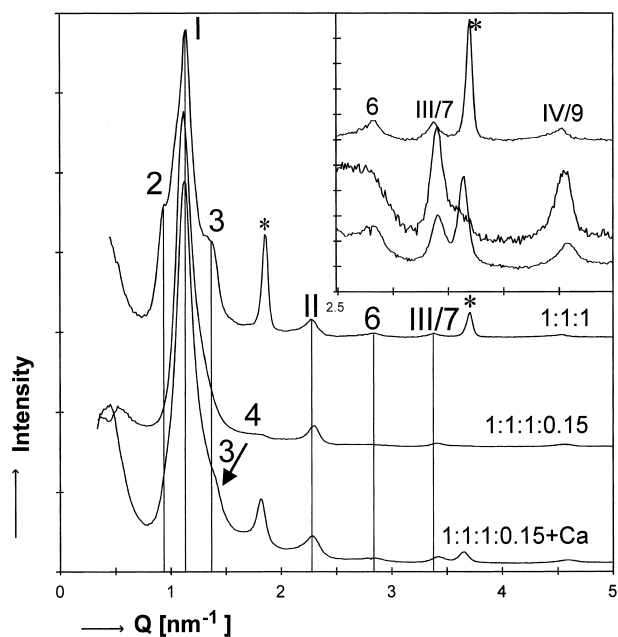*CHOL:HCER:FFA mixtures at increased temperature.* The phase

Fig. 5. The phase behavior of equimolar CHOL:HCER:FFA mixtures (1:1:1) in the absence and presence of cholesterol sulfate (1:1:1:0.15) and calcium (1:1:1:0.15+Ca) at pH 5. The Arabic numbers indicate the diffraction orders of the LPP (repeat distance, 13.0 nm). The Roman numbers indicate the diffraction orders of the SPP (repeat distance, 5.5 or 5.6 nm). The 5.5 and 5.6 nm phases are characterized by peaks with spacing at 5.5 nm ($Q = 1.14$ nm^{-1}, first order), 2.77 nm ($Q = 2.26$ nm^{-1}, second order), 1.85 nm ($Q = 3.40$ nm^{-1}, third order), and 1.35 nm ($Q = 4.65$ nm^{-1}, fourth order). The two shoulders on both sides of the 5.5 nm peak with spacings of 6.2 nm ($Q = 1.01$ nm^{-1}, second order) and 4.5 nm ($Q = 1.39$ nm^{-1}, third order) are attributed to the 13 nm phase. In addition, the 2.23 nm peak ($Q = 2.81$ nm^{-1}) is a sixth order reflection of the 13 nm phase. Addition of cholesterol sulfate reduces the intensity of the peaks attributed to the 13.0 nm lamellar phase. On the basis of the broad 3.4 nm ($Q = 1.84$ nm^{-1}, fourth order), 2.31 nm ($Q = 2.72$ nm^{-1} sixth order), and 1.85 nm ($Q = 3.40$ nm^{-1}, seventh order) reflections, it is likely that a small fraction of the lipids forms the 13 nm lamellar phase. Addition of calcium (Ca) results in a detection of the third order of the 13.0 nm lamellar phase (see arrow). An asterisk indicates a reflection attributed to crystalline CHOL at a spacing of 3.33 nm ($Q = 1.86$ nm^{-1}) and 1.69 nm ($Q = 3.74$ nm^{-1}).

behavior of the equimolar CHOL:HCER:FFA mixture has been examined in the temperature range between 25°C and 95°C (**Fig. 6**). Each curve represents the lipid phase behavior during a 2°C rise in temperature. The phase behavior at room temperature is similar to that shown in Fig. 5. Two lamellar phases with periodicities of 13 and 5.7 nm have been observed. An increase in temperature does not change the phase behavior dramatically until a temperature of 53°C is reached. At that temperature the peak indicated as being third order of the 13 nm phase increases in intensity, while the 5.7 nm peak (first order SPP) decreases in intensity. As observed for pigCER mixtures, a new phase is formed in this temperature region with a periodicity of approximately 4.25 nm, which is slightly shorter than the third order peak spacing of the 13 nm phase. A further increase in temperature increases the intensity of this peak dramatically, while the peaks attributed to the LPP and
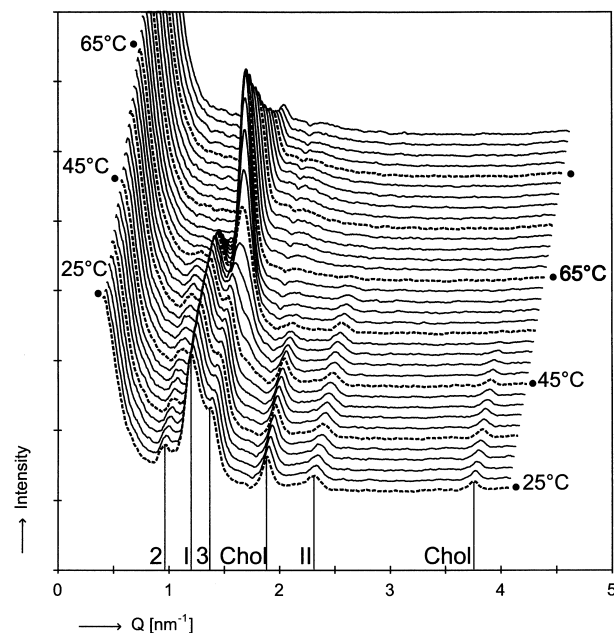

Fig. 6. Changes in the lipid phase behavior of CHOL:HCER:FFA mixtures as a function of temperature. The mixtures were prepared at pH 5. The Arabic numbers indicate the diffraction orders of the long periodicity lamellar phase (repeat distance varies by 13 nm). The Roman numbers refer to the diffraction peaks attributed to the SPP (repeat distance varies between 5.7 nm). Each diffraction curve represents the scattered X-rays during a temperature rise of 2°C. The dashed lines represent the diffraction curves at 25, 35, 55, 65, 75, and 85°C.

SPP disappear at 67°C and 69°C, respectively. At about 63°C the peak attributed to the SPP starts to shift to smaller Q values.

DISCUSSION

In the present study the lipid phase behavior of mixtures prepared with HCER isolated from human SC has been examined, with the main focus being on the role of major lipid classes (CHOL, HCER, and FFA) on lipid phase behavior. In addition, we have also examined the effect of cholesterol sulfate. The results summarized in **Fig. 7** and **Tables 1** and **2** indicate that *i*) in CHOL:HCER mixtures the LPP dominates, hexagonal lateral packing is formed, and a small fraction of lipids forms a fluid phase; *ii*) in CHOL:HCER:FFA mixtures the SPP is dominant. Furthermore, the lateral packing is mainly orthorhombic. The liquid packing is more prominently present than in CHOL:HCER mixtures; *iii*) in an equimolar CHOL:HCER(2–8) mixture only a small fraction of lipids forms the LPP and a lamellar phase with a periodicity of 5.3 nm (referred to as SPP) is predominant; and *iv*) addition of cholesterol sulfate to CHOL:HCER:FFA mixtures does not affect the phase behavior markedly, except for an increased solubility of cholesterol in the lipid lamellar phases.

The lipid phase behavior summarized above differed in a number of features from that seen in the mixtures prepared with pigCER. These differences are highlighted below.
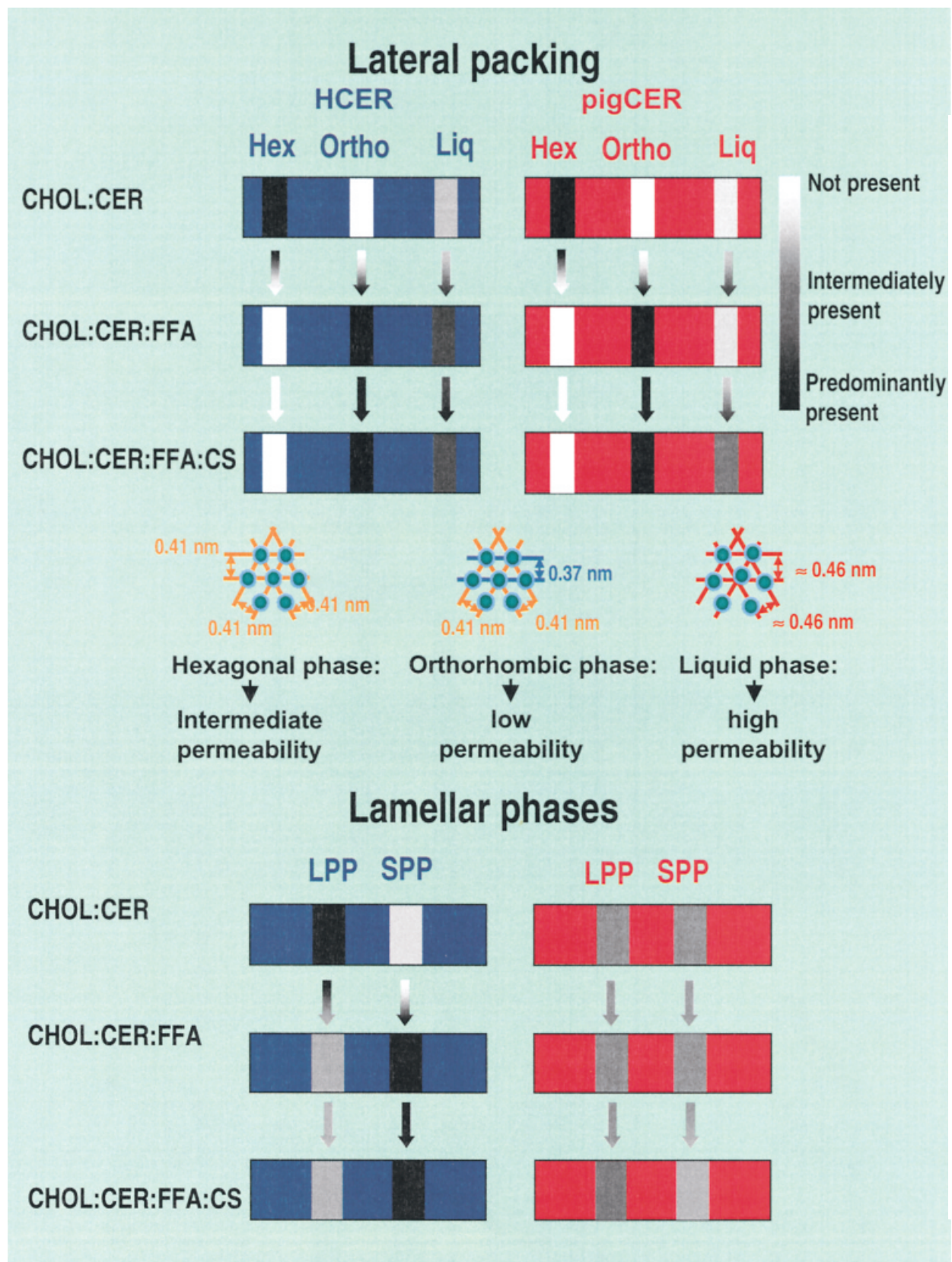
Fig. 7. The lateral and lamellar phases in equimolar CHOL:HCER and CHOL:HCER:FFA mixtures and in CHOL:HCER:FFA:CS (1:1:1:0.15) mixtures are compared with those prepared with pigCER. The molecular arrangements of the liquid, hexagonal, and orthor-hombic lateral packing are presented schematically. The liquid lateral packing is prevalent in equimolar CHOL:HCER:FFA mixtures as compared with CHOL:HCER mixtures, whereas in pigCER-containing mixtures the liquid phase is obviously present only after addition of cholesterol sulfate (CS). The LPP is more prominently present in CHOL:HCER mixtures than in CHOL:HCER:FFA mixtures. In the case of pigCER-containing mixtures addition of FFA does not affect the formation of the lamellar phases.

TABLE 1. Lateral packing of lipid mixtures

Composition	Molar Ratio	Hex	Ortho	Liquid	CHOL
CHOL:HCER	0.2:1	+	−	−	−
	0.6:1	+	−	±	±
	1:1	+	−	±	+
CHOL:HCER(2–8)	1:1	+	−	−	+
CHOL:HCER:FFA	1:1:1	−	+	+	±
	1:1:1 (pH 7.4)	−	+	+	±
	1:1:0.8	−	+	+	+
	1:1:0.6	−	+	+	+
	1:1:0.4	−	+	±[a]	+
CHOL:HCER:FFA/PA	1:1:1 (50/50)	−	+	+	+
CHOL:HCER:FFA:CS	1:1:1:0.15	−	+	+	±
	1:1:1:0.15 (pH 7.4)	−	+	+	±
	1:1:1:0.3	−	+	+	±
	1:1:1:0.15 + Ca	−	+	+	±

Abbreviations: Hex, Hexagonal lateral packing; Ortho, orthorhombic lateral packing; CS, cholesterol sulfate; +, strongly present; ±, weakly present; −, not present; CHOL, cholesterol; HCER, human ceramide; PH, palmitic acid.

[a] Liquid phase difficult to identify because of the presence of cholesterol reflections.

Comparison between mixtures prepared from either pigCER or HCER

Previous studies (13, 14, 16) and the present study reveal that in CHOL:CER mixtures prepared with both pig and human CER the following similarities in phase behavior have been observed: *a*) In CHOL:CER mixtures the LPP is formed, demonstrating the formation of the same lamellar phases as present in intact SC; *b*) the phase behavior of CHOL:CER mixtures is not sensitive to changes in the CHOL:CER molar ratio over a wide range; *c*) in CHOL:CER mixtures hexagonal lateral packing is present. Addition of long chain FFA induces a transition from hexagonal to orthorhombic lateral packing; *d*) the presence of cholesterol sulfate increases the solubility of CHOL in CHOL:CER:FFA mixtures; and *e*) in mixtures prepared with HCER lacking HCER1 the formation of the LPP is strongly reduced, as observed with pigCER mixtures.

Besides these important similarities, some differences in phase behavior between lipid mixtures based on pigCER and HCER have also been noticed: *i*) In the diffraction patterns of mixtures prepared from CHOL: HCER:FFA the presence of a broad peak that can be attributed to liquid lateral packing is obvious, whereas in CHOL:pigCER:FFA mixtures liquid packing is obvious only after addition of cholesterol sulfate; *ii*) the phase behavior of the equimolar CHOL:HCER:FFA mixtures differs from that of the equimolar CHOL:pigCER:FFA mixtures. As can be deduced from Figs. 4A and 5, in the presence of FFA the intensities of the peaks attributed to the LPP in mixtures based on HCER are reduced and the peaks are broader than in the patterns of the CHOL: pigCER mixtures. This indicates that, in contrast to the situation with pig SC lipids, addition of FFA not only induces the formation of orthorhombic lateral packing, but also decreases the amount of

TABLE 2. Lamellar phases and crystalline CHOL in the lipid mixtures

Composition	Molar Ratio	LPP	SPP	CHOL
CHOL:HCER	0.2:1	12.8 (1,2,3,4,6,7)	5.4 (2,7)?	−
	0.6:1	12.8 (1,2,3,6,7)	5.4 (2,7)?	+
	1:1	12.8 (1,2,3,6,7)	5.4 (2,7)?	+
CHOL:HCER(2–8)	1:1	12.8 (2,3), weak	5.4 (1,2)	+
CHOL:HCER:FFA	1:1:1	13 (2,3,6)	5.5 (1,2,3,4)	+
	1:1:1 (pH 7.4)	13 (3)?	5.7 (1,2,3,4)	+
	1:1:0.8	13 (2,3,6)	5.5 (1,2,3,4)	+
	1:1:0.4	13 (2,3,6)	5.5 (1,2,3,4)	+
CHOL:HCER:FFA:CS	1:1:1:0.15	13 (4,6)	5.6 (1,2,3,4)[a]	−
	1:1:1:0.15 (pH = 7.4)	13 (3,4)	5.7 (1,2,3,4)	−
	1:1:1:0.15 + Ca	13 (2,3,4,6)	5.6 (1,2,3,4)[a]	−
	1:1:1:0.15 + Ca (pH 7.4)	12 (3,4,6)	5.7 (1,2,3,4)	−

Abbreviations: LPP, long periodicity lamellar phase; SPP, short periodicity phase. A question mark indicates that the presence of this phase is uncertain. CS, Cholesterol sulfate; CHOL, cholesterol; +, strongly present; ±, weakly present; − not present; 12.8 (1,2,3,4,6,7) means periodicity is 12.8 nm, interpretation is based on the presence of the first, second, third, fourth, sixth, and seventh order reflections.

[a] The presence of a broad, strong peak at 5.6 nm spacing clearly shows that a large fraction of lipids forms the short SPP. However, the LPP is still present as indicated by the broad peaks at 3.3 and 2.2 nm (fourth and sixth order of this phase). Most probably the second and third order peaks of the LPP are weaker and broad and therefore cannot be distinguished from the broad 5.6 nm peak.

lipid that forms the LPP. The increase in width at half-peak intensity indicates either increased thermal mobility or increased lattice disorder. The increase in thermal mobility lattice disorder is in contrast to the formation of a crystalline phase. However, it is possible that increased lattice disorder might be related to the more prominent presence of the liquid phase in CHOL:HCER:FFA mixtures in comparison with HCER: CHOL and CHOL: pigCER:FFA mixtures; *iii*) in the diffraction patterns of equimolar CHOL:pigCER:FFA mixtures strong reflections attributed to CHOL were present, whereas in the corresponding CHOL:HCER:FFA mixtures the CHOL reflections are much weaker. From this observation it is clear that a larger fraction of CHOL can be intercalated in lamellar phases of the HCER-containing lipid mixtures than in the lamellar phases formed in mixtures prepared with pigCER. This increased solubility of CHOL in the lamellae might be related to the presence of a liquid sublattice. This difference in solubility of CHOL has also been observed in human SC. In pig SC phase-separated crystalline CHOL has always been detected (4), whereas in human SC only 50% of SC samples has phase-separated crystalline CHOL been detected; *iv*) in previous studies with CHOL:pigCER mixtures two lamellar phases with periodicities of 5.2 nm (SPP) and 12.2 nm (referred to as LPP) have clearly been detected. The diffraction curves of the CHOL:HCER mixtures show that the 13 nm lamellar phase (LPP) is more dominantly present than in the CHOL:pigCER mixtures (see Fig. 7). The formation of the SPP is not obvious; and *v*) whereas in mixtures based on pigCER cholesterol sulfate promotes the formation of the LPP, addition of cholesterol sulfate to equimolar CHOL:HCER:FFA mixtures promotes the formation of the SPP.

From the results described in this article, it is obvious that the phase behavior of lipid mixtures prepared with HCER and of mixtures prepared with pigCER differ in some aspects. In a study carried out simultaneously with the present study (28) the formation of the liquid phase has been related to the presence of the unsaturated acyl chain linked to the ω-hydroxy fatty acid chain in the CER mixture (28, 29). Furthermore, in that study it was suggested that for the formation of the LPP a certain (optimal) fraction of lipids must form a liquid phase. When the fraction forming this liquid phase is either too low or too high, the formation of the SPP is increased at the expense of the formation of the LPP. The relationship between the fraction of lipids forming a fluid phase and the formation of the LPP might explain the differences in phase behavior between mixtures prepared from pigCER and HCER. Namely, because the fraction of CER containing linoleic acid linked to ω-hydroxy fatty acid in the HCER (HCER1 and HCER4) mixture is higher (18%, w/w) than in the pigCER mixture (8%, w/w) (13), one can expect in mixtures based on HCER a strong increase in the formation of the liquid phase. This has indeed been clearly observed for the CHOL:HCER:FFA mixtures. The presence of a high fraction of liquid phase might prevent the formation of the LPP in CHOL:HCER:FFA mixtures. In contrast, in

CHOL:pigCER:FFA mixtures the presence of the fluid phase is less prominent, which favors the formation of the LPP. Addition of cholesterol sulfate to CHOL:HCER: FFA mixtures might increase the formation of the fluid phase even further (as observed in pigCER mixtures) and therefore reduce the formation of the LPP, which indeed has been observed in the present study. However, it must be realized that in the in vivo situation the fraction of HCER1 and HCER4 between different donors may strongly vary, being between 8% and 18% (w/w) (30). As a consequence, reduction of the HCER1+HCER4 content might result in phase behavior similar to that observed with mixtures based on pigCER.

Phase behavior of HCER:CHOL mixtures at elevated temperatures

When comparing the presence of lamellar phases and lateral packing as function of temperature, some interesting conclusions can be made. Between 20°C and 32°C a transition of orthorhombic to hexagonal lateral packing occurs, whereas no changes in lamellar phase behavior have been noticed. This suggests that in this temperature range the orthorhombic-hexagonal phase transition does not affect the lamellar phase behavior. However, at elevated temperatures the situation changes. There, the LPP disappears between 61°C and 69°C (see Fig. 6), indicating the existence of a relationship between the formation of a fluid phase and the presence of the LPP. This occurs exactly in the same temperature range in which the hexagonal lateral packing is transformed to liquid phase (Fig. 3). Furthermore, a new phase with a periodicity of 4.3 nm is formed at elevated temperatures. Such a phase was also found in mixtures prepared with pigCER. This phase was less prominent or even absent in intact SC. From the experiments performed with mixtures prepared from pigCER it became clear that the fraction of lipids forming this phase at elevated temperatures decreased when at room temperature the amount of phase-separated CHOL was reduced (16). Such a situation can also be achieved by addition of cholesterol sulfate.

Molecular arrangement and permeation

On the basis of results obtained with mixtures based on pigCER and HCER we have proposed a "sandwich" model for molecular arrangement of lipids in the LPP (28, 29). In this model the lipids in the LPP are arranged in two broad crystalline lipid layers, between which a narrow central lipid layer with a subpopulation of lipids forming fluid domains or channels is located (see **Fig. 8**). In this central layer the linoleic acid moiety of CER1 is located. Because the CHOL:pigCER mixtures are less fluid than the CHOL: HCER mixtures, one can speculate that the lower mobility in CHOL:pigCER mixtures will prevent the formation of the fluid central layer and thus the formation of the LPP, because the adjacent broad crystalline lipid layers are too crystalline (strong van der Waals interactions) to allow the formation of a fluid phase. The presence of a fluid phase will strongly increase the mobility of the lattice, as is expected to occur in HCER mixtures. It is probably a result
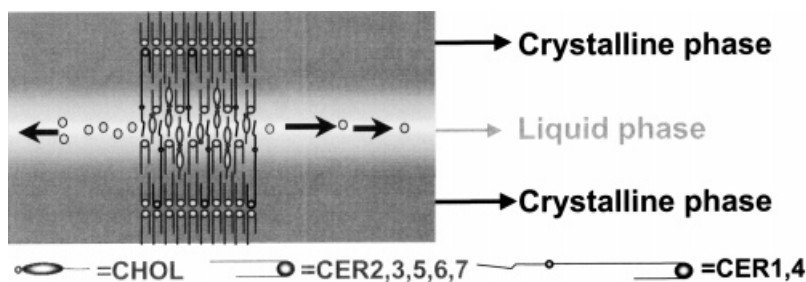
Fig. 8. The molecular arrangement of the LPP in HCER:CHOL mixtures. In accordance with this model the repeating unit in the structure consists of three lipid layers. In the central layer the unsaturated linoleic moieties of HCER1 and HCER4 are located. On the basis of the molecular model we proposed the "sandwich model." The liquid phase is located in domains or in continuous channels in the central lipid layer of this phase. In the sublattice adjacent to the central layer a gradual change in lipid mobility occurs because of the presence of less mobile long saturated hydrocarbon chains. This gradual change to crystalline packed lipid layers on both sides of the central layer avoids the formation of new interfaces. The highest permeability is expected to be located parallel to the basal plane of the lamellae in the fluid domains.

of the presence of HCER1 and HCER4 in more conformations (achieved by the rotation or twisting of single bonds) than the conformation required for the formation of the LPP. This might be the reason that a strong increase in the lattice mobility prevents the formation of the LPP in CHOL:HCER:FFA mixtures. Speculations about the consequences of this model for permeability have been discussed extensively in a related article (28). Briefly, it is generally accepted that fluid phases have a much higher permeability (and often solubility) than crystalline phases. If the fluid phase is localized in the central layer in the LPP, permeation in the fluid phase parallel to the basal plane of the lamellae would be much faster than permeation perpendicular to the lamellae (across the head group regions). This will also facilitate communication between desmosomes. An increase in the fraction of unsaturated acyl chains linked to the long base ω-hydroxy group would increase the fluidity and thus the permeability, particularly in the plane parallel to the basal plane. If indeed the two broad lipid layers adjacent to the central narrow layer are mainly crystalline, permeation perpendicular to the basal plane is most probably the rate-limiting step. In this direction permeation should occur either through the crystalline domains, or along boundaries of crystal imperfection and/or along boundaries of neighboring lamellar domains. Permeation between the boundary of a lamellar sheet and the neighboring desmosome might also be possible.

In vivo lipid organization

When extrapolating our findings to the in vivo situation, some remarks can be made. According to our results it is expected that in human SC a liquid phase is present in the intercellular lipid lamellae. The presence of a subpopulation of lipids forming a liquid phase is in agreement with previous FTIR experiments (15) carried out with intact human SC, but could not be detected by the X-ray diffraction technique because of the presence of keratin (6). Furthermore the formation of the LPP in the equimolar CHOL:HCER:FFA mixtures is less prominent than in SC, in which frequently the third order of the LPP

is clearly present. The reduced LPP content in the mixtures based on HCER might be caused by the high HCER1+HCER4 content. Our results further suggest that the presence of HCER1 in CHOL:HCER mixtures is a requirement for the formation of the LPP. From this observation we conclude that, as in mixtures prepared with pigCER (7), HCER1 plays an important role in the formation of the LPP. This means that in vivo a reduction of HCER1 content, as found in atopic dermatitis patients or dry skin (31), may lead to alteration of the organization of lamellar phases. Indeed, a relationship between a reduced HCER1 level and a reduction of the LPP has also been observed in vivo (32). However, as has become clear in this and a related study (28), in those cases, when a sufficient amount of HCER1 is present to form the LPP, the formation of the LPP can be reduced by the presence of a liquid phase. Such a situation may occur in X-linked ichthyosis patients, who have a strongly elevated level of cholesterol sulfate (10%, w/w) in the SC (33). It can be speculated that a high amount of cholesterol sulfate promotes the formation of a fluid phase to such an extent that a reduction in the formation of the LPP can be expected. A strong increase in the formation of the liquid phase is observed after adding only 2% cholesterol sulfate to CHOL:pigCER:FFA mixtures. In the present study the promotion of a liquid phase was less obvious, probably because of the high level of HCER1+HCER4 that had already induced a liquid phase in CHOL:HCER:FFA mixtures. Finally, in lamellar ichthyosis patients a reduction in FFA:HCER and FFA:CHOL molar ratio has been observed (34). Furthermore, it has been shown that the hexagonal lattice in these patients is more prominently present at the expense of the orthorhombic sublattice (35). In the present study, it is shown that lipids in CHOL:HCER mixtures form a hexagonal lateral packing, but that at strongly reduced FFA:CHOL and FFA:HCER molar ratios the orthorhombic phase is still prominently present. Therefore, it can be speculated that the reduced FFA content observed in X-linked ichthyosis patients will affect the lateral packing, but is not the only factor explaining the prominent presence of the hexagonal sublattice. Possibly other factors, such as a re-

duced hydrocarbon chain length of FFA and of CER, may play an important role as well.▮

REFERENCES

1. White, S. H., D. Mirejovsky, and G. I. King. 1988. Structure of lamellar lipid domains and corneocyte envelopes of murine stratum corneum. An X-ray diffraction study. *Biochemistry.* **27:** 3725–3732.
2. Bouwstra, J. A., G. S. Gooris, J. A. van der Spek, and W. Bras. 1991. Structural investigations of human stratum corneum by small-angle X-ray scattering. *J. Invest. Dermatol.* **97:** 1005–1012.
3. Bouwstra, J. A., G. S. Gooris, J. A. van der Spek, S. Lavrijsen, and W. Bras. 1994. The lipid and protein structure of mouse stratum corneum: a wide and small angle diffraction study. *Biochim. Biophys. Acta.* **1212:** 183–192.
4. Bouwstra, J. A., G. S. Gooris, W. Bras, and D. T. Downing. 1995. Lipid organization in pig stratum corneum. *J. Lipid Res.* **36:** 685–695.
5. Garson, J-C., J. C. Doucet, J-L. Lévêque, and G. Tsoucaris. 1991. Oriented structure in human statum corneum revealed by X-ray diffraction. *J. Invest. Dermatol.* **96:** 43–49.
6. Bouwstra, J. A., G. S. Gooris, M. A. Salomons-de Vries, J. A. van der Spek, and W. Bras. 1992. Structure of human stratum corneum as a function of temperature and hydration: a wide-angle X-ray diffraction study. *Int. J. Pharm.* **84:** 205–216.
7. Bouwstra, J. A., G. S. Gooris, F. E. R. Dubbelaar, A. M. Weerheim, A. P. Ijzerman, and M. Ponec. 1998. The role of ceramide 1 in the molecular organisation of SC lipids. *J. Lipid Res.* **39:** 186–196.
8. Kitson, N., J. Thewalt, M. Lafleur, and M. Bloom. 1994. A model membrane approach to the epidermal permeability barrier. *Biochemistry.* **33:** 6707–6715.
9. Fenske, D. B., J. L. Thewalt, M. Bloom, and N. Kitson. 1994. Models of stratum corneum intercellular membranes: ^{2}H NMR of microscopically oriented multilayers. *Biophys. J.* **67:** 1562–1573.
10. Bouwstra, J. A., J. Thewalt, G. S. Gooris, and N. Kitson. 1997. A model membrane approach to the epidermal permeability barrier: an X-ray diffraction study. *Biochemistry.* **36:** 7717–7725.
11. Moore, D. J., M. E. Rerek, and R. Mendelsohn. 1997. Lipid domains and FTIR spectroscopy studies of the conformational order and phase behaviour of ceramides. *J. Phys. Chem.* **101:** 8933–8940.
12. Moore, D. J., and M. E. Rerek. 2000. Insights into the molecular organisation of lipids in the skin barrier from infrared spectroscopy studies of stratum corneum lipid models. *Acta Derm. Venereol. Suppl. (Stockh.).* **208:** 16–22.
13. Bouwstra, J. A., G. S. Gooris, K. Cheng, A. Weerheim, W. Bras, and M. Ponec. 1996. Phase behavior of isolated skin lipids. *J. Lipid Res.* **37:** 999–1011.
14. Bouwstra, J. A., G. S. Gooris, F. E. R. Dubbelaar, A. Weerheim, and M. Ponec. 1998. pH, cholesterol sulfate and fatty acids affect stratum corneum lipid organisation. *J. Invest. Dermatol. Proc.* **3:** 69–74.
15. Gay, C. L., R. H. Guy, G. M. Golden, V. M. Mak, and M. L. Francoeur. 1994. Characterization of low-temperature (i.e., <65°C) lipid transitions in human stratum corneum. *J. Invest Dermatol.* **103:** 233–239.
16. Bouwstra, J. A., G. S. Gooris, F. E. R. Dubbelaar, A. Weerheim, and M. Ponec. 1999. Cholesterol sulfate and calcium affect stratum corneum lipid organisation over a wide temperature range. *J. Lipid Res.* **40:** 2303–2312.
17. Aly, R., C. Shirley, B. Cumico, and H. I. Maibach. 1978. Effect of prolonged occlusion on the microbial flora, pH, carbon dioxide and transepidermal water loss on human skin. *J. Invest. Dermatol.* **71:** 378–381.
18. Sage, B. H., R. H. Huke, A. C. McFarland, and K. Kowalczyk. 1993. The importance of skin pH in iontophoresis of peptides. *In* Prediction of Percutaneous Penetration. K. Brain, V. James, and K. A. Walters, editors. STS Publishing, Cardiff. 410–418.
19. Turner, N., C. Cullander, and R. H. Guy. 1998. Determination of the pH gradient across the stratum corneum. *J. Invest. Dermatol. Symp. Proc.* **3:** 110–113.
20. Robson, K. J., M. E. Stewart, S. Michelsen, N. D. Lazo, and D. T. Downing. 1994. 6-Hydroxy-4-sphingenine in human epidermal ceramides. *J. Lipid Res.* **35:** 2060–2068.
21. Stewart, M., and D. T. Downing. 1999. A new 6-hydroxy-4-sphinganine containing ceramide in human skin. *J. Lipid Res.* **40:** 1434–1439.
22. Wertz, P. W., and D. T. Downing. 1983. Ceramides of pig stratum epidermis, structure determination. *J. Lipid Res.* **24:** 753–758.
23. Bligh, E. G., and W. J. Dyer. 1959. A rapid method of total lipid extraction and purification. *Can. J. Biochem. Physiol.* **37:** 911–917.
24. Ponec, M., A. Weerheim, J. Kempenaar, A. M. Mommaas, and D. H. Nugteren. 1988. Lipid composition of cultured human keratinocytes in relation to their differentiation. *J. Lipid Res.* **29:** 949–962.
25. Wertz, P. W., and D. T. Downing. 1991. *In* Physiology, Biochemistry, and Molecular Biology of the Skin. 2nd edition. L. A. Goldsmith, editor. Oxford University Press, New York. 205–236.
26. Small, D. 1986. Handbook of Lipid Research 4: The Physical Chemistry of Lipids. D. Small, editor. Plenum Press, New York. 183.
27. Pilgram, G. S. K., A. M. Engelsma-van Pelt, J. A. Bouwstra, and H. K. Koerten. 1999. Electron diffraction provides new information on human stratum corneum lipid organization in relation to depth and temperature. *J. Invest. Dermatol.* **113:** 403–409.
28. Bouwstra, J. A., G. S. Gooris, F. E. R. Dubbelaar, A. Weerheim, and M. Ponec. 2001. Phase behavior of stratum corneum lipid mixtures based on human ceramides: the role of natural and synthetic ceramide 1. *J. Invest. Dermatol.* In press.
29. Bouwstra, J. A., G. S. Gooris, F. E. R. Dubbelaar, and M. Ponec. 2000. The lipid organisation in the skin barrier. *Acta Derm. Venereol. Suppl. (Stockh.).* **208:** 23–30.
30. Weerheim, A. M., and M. Ponec. 2001. Determination of stratum corneum lipid profile by tape stripping in combination with high-performance thin-layer chromatography. *Arch Dermatol. Res.* **293:** 191–199.
31. Imokawa, G., A. Abe, M. Kawashima, and A. Hidano. 1991. Decreased levels of ceramides in stratum corneum of atopid dermatitis: an etiologic factor in atopic dry skin? *J. Invest. Dermatol.* **96:** 523–526.
32. Schreiner, V., G. S. Gooris, S. Pfeiffer, G. Lanzendorfer, H. Wenck, W. Diembeck, E. Proksch, and J. A. Bouwstra. 2000. Barrier characteristics of different human skin types investigated with X-ray diffraction, lipid analysis and electron microscopy imaging. *J. Invest. Dermatol.* **114:** 654–660.
33. Elias, P. M., M. L. Williams, M. E. Maloney, J. A. Bonifas, B. E. Brown, S. Grayson, and E. H. Epstein. 1984. Stratum corneum lipids in disorders of cornification. *J. Clin. Invest.* **74:** 1414–1421.
34. Lavrijsen, A. P. M., J. A. Bouwstra, G. S. Gooris, H. E. Boddé, and M. Ponec. 1995. Reduced skin barrier function parallels abnormal stratum corneum lipid organisation in patients with lamellar ichthyosis. *J. Invest. Dermatol.* **105:** 619–624.
35. Pilgram, G. S. K., D. C. J. Vissers, H. van der Meulen, S. Pavel., S. P. M. Lavrijsen, J. A., Bouwstra, and H. K. Koerten. 2001. Abberant lipid organization in stratum corneum of patients with atopic dermatitis and lamellar ichthhyosis. *J. Invest. Dermatol.* In press.